

Article

## Long Alkyl Chain Organophosphorus Coupling Agents for *in Situ* Surface Functionalization by Reactive Milling

Annika Betke and Guido Kickelbick \*

Inorganic Chemistry, Saarland University, Am Markt Zeile 3, Saarbrücken 66125, Germany;  
E-Mail: annika.betke@uni-saarland.de

\* Author to whom correspondence should be addressed; E-Mail: guido.kickelbick@uni-saarland.de;  
Tel.: +49-0-681-302 (ext. 70651); Fax: +49-0-681-302 (ext. 70652).

Received: 8 May 2014; in revised form: 2 July 2014 / Accepted: 14 July 2014 /

Published: 4 August 2014

---

**Abstract:** Innovative synthetic approaches should be simple and environmentally friendly. Here, we present the surface modification of inorganic submicrometer particles with long alkyl chain organophosphorus coupling agents without the need of a solvent, which makes the technique environmentally friendly. In addition, it is of great benefit to realize two goals in one step: size reduction and, simultaneously, surface functionalization. A top-down approach for the synthesis of metal oxide particles with *in situ* surface functionalization is used to modify titania with long alkyl chain organophosphorus coupling agents. A high energy planetary ball mill was used to perform reactive milling using titania as inorganic pigment and long alkyl chain organophosphorus coupling agents like dodecyl and octadecyl phosphonic acid. The final products were characterized by IR, NMR and X-ray fluorescence spectroscopy, thermal and elemental analysis as well as by X-ray powder diffraction and scanning electron microscopy. The process entailed a tribochemical phase transformation from the starting material anatase to a high-pressure modification of titania and the thermodynamically more stable rutile depending on the process parameters. Furthermore, the particles show sizes between 100 nm and 300 nm and a degree of surface coverage up to 0.8 mmol phosphonate per gram.

**Keywords:** reactive milling; titania particles; long alkyl chain organophosphorus coupling agents; tribochemical phase transition

---

## 1. Introduction

Surface modified particles are important building blocks for various applications in optics [1], electronics [2], material science [3] and in the biomedical field [4]. For this reason, there is increasing interest in economic synthetic strategies. In this context, there has been significant interest in mechanochemical approaches [5,6]. Reactive milling turned out to be a promising technique because it is a solvent-free and environmentally friendly alternative to conventional synthetic strategies [7,8]. Reactive milling has proven its suitability for the synthesis of various materials, for example calcium hydride by reactive milling of calcium and phenylphosphonic acid (PPA) under an inert atmosphere [9] or  $ZrTiO_4$  [10] to name only two examples out of many others. Recently, we investigated the suitability of reactive milling for the preparation of surface functionalized titania nanoparticles. We were able to show that an *in situ* surface functionalization using PPA as coupling agent is possible and that the organophosphorus surface functionalization can stabilize crystallographic high-pressure phases [11,12]. Often the surface functionalization of particles with organic coupling agents involves the use of organic solvents; our technique allows a solvent free, ecologically more friendly approach. In case of PPA, the surface functionalization of titania can also be obtained in water as solvent [13]. This is not the case for long alkyl chain phosphonic acids. Here, definitely an organic solvent is necessary for the complete dissolution of the respective coupling agent [14,15]. This was the reason for us to expand our previous studies to this type of surface modifier. Dodecylphosphonic acid (DDPA) was used to perform a systematic study on the behavior at different process parameters. Afterwards, octadecylphosphonic acid (ODPA) was used to demonstrate that the approach is assignable on other long alkyl chain organophosphorus species.

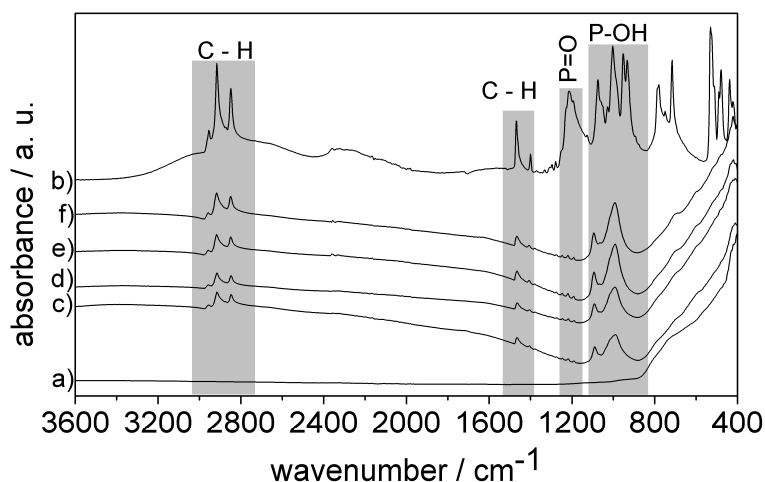
## 2. Results and Discussion

Reactive milling was carried out using titania as inorganic pigment and long alkyl chain organophosphorus coupling agents. The experiments were performed in a high-energy planetary ball mill using a  $ZrO_2$ -ceramic grinding bowl and varying the reaction conditions such as milling time and rotational speed (revolutions per minute, rpm). Titania has several crystallographic phases that can be converted into each other depending on the energy input into the system. Consequently, the ratio between the different crystallographic phases is an indicator for the energy applied to the samples. After the milling process, the obtained material was thoroughly washed and dried. The washing solution was analyzed to demonstrate that the coupling agent is not degraded due to the high-energy impact during the milling process.  $^1H$ ,  $^{13}C$  and  $^{31}P$  NMR spectra confirm that DDPA was the only species present in the washing solution (see Supplementary Information Figures S1–S6).

The final products were analyzed applying various techniques. A systematic study on the influence of different process parameters was performed for the DDPA functionalized particles. FTIR analyses show that the milling process results in a bonding between the coupling agent and the titania phase. The starting material reveals no absorption in the typical regions for organic molecules. In contrast, the samples after the milling process display bands that are characteristic for C–H vibrations ( $2900\text{ cm}^{-1}$  and  $1450\text{ cm}^{-1}$ ) as well as P–O oscillations ( $1000\text{ cm}^{-1}$ ) (Figure 1 and Supplementary Information Figures S7 and S8). The broad band at approximately  $1000\text{ cm}^{-1}$  is characteristic for surface bonded

phosphonates; the width of this band is due to the different bonding types (e.g., bi- and tridentate) of the phosphonates on the titania surface [16].

**Figure 1.** FTIR-spectra: (a) starting material titania; (b) coupling agent dodecylphosphonic acid and samples after the milling process: (c) 300 rpm/12 h; (d) 300 rpm/24 h; (e) 300 rpm/36 h; (f) 300 rpm/48 h; surface modification has taken place after the milling process, which is indicated by the characteristic bands for the C–H oscillation ( $1450\text{ cm}^{-1}$  and  $2900\text{ cm}^{-1}$ ) and the wide band at  $1000\text{ cm}^{-1}$  (P–O region).



To determine the amount of surface coverage, thermal gravimetric (TGA) and elemental (CHN) analyses were performed and the results were correlated with the process parameters rotational speed and milling time (Figure 2). It turned out that the degree of surface coverage increases with increasing milling time as well as increasing milling speed. This correlation can have two reasons. On the one hand, a better binding of the organic groups to the titania surface can have its origin in the increased energy input. On the other hand, the surface area of the particles is increased which could lead to a higher portion of coupling agent bound to the surface. The results show that the correlation between the surface coverage and the milling time or speed is almost linear. CHN and TGA results show similar development, the slight discrepancies are due to measuring inaccuracies of both methods.

The binding modes of the DDPA to the titania surface were studied by the use of solid-state NMR spectroscopy. The results reveal that DDPA was bonded to the titania surface. Pure DDPA yields in a solid-state  $^{31}\text{P}$  NMR signal at  $\delta = 31.9\text{ ppm}$  [17], whereas the samples after the milling process show a series of partially broad signals in the range of  $\delta = 10\text{--}35\text{ ppm}$ . Furthermore, a sharp peak is observed at  $\delta = 11\text{ ppm}$  (Figure 3 and Supplementary Information Figures S9–S12). This is in good agreement with the variety of possible binding modes of the phosphonate to the metal oxide surface. In literature, for tridentate coordination modes, sharp peaks with chemical shifts of around 20 ppm to lower fields with respect to the free phosphonic acid are reported [18]. For bi- and monodentate binding modes the downfield shift is less pronounced and the corresponding peaks are significantly broader [19]. Consequently, the peaks in the range of 10–35 ppm correspond to the bi- and monodentate bonded phosphonates and the sharp signal at around 11 ppm can be assigned to the tridentate coordinated species for the samples obtained by reactive milling of titania with DDPA. Theoretically, the signal for tridentate phosphonate species at around 11 ppm could be attributed to layered bulk titanium

alkylphosphonates [19]. However, these species show a significantly increased decomposition temperature ( $\sim 750$  °C) compared to alkyl phosphonate modified titania nanoparticles ( $\sim 550$  °C) represented by an additional exothermic step in TG measurements. The TG measurements of the samples obtained by reactive milling of titania with DDPA clearly show only one decomposition step for the degradation of phosphonate species at around 550 °C (Figure 4). Therefore, the presence of layered titanium phosphonate compounds can be excluded [19]. The solid-state  $^{13}\text{C}$  NMR spectra of all samples show signals in the alkyl chain region at  $\delta = 5\text{--}30$  ppm which reveals that the alkyl chain is still present after the milling process (Figure 3 and Supplementary Information Figures S9–S12).

**Figure 2.** Surface modification in dependence of (a) the rpm or (b) the milling time, results calculated from TG analyses (straight line) and from CHN analyses (dashed line).

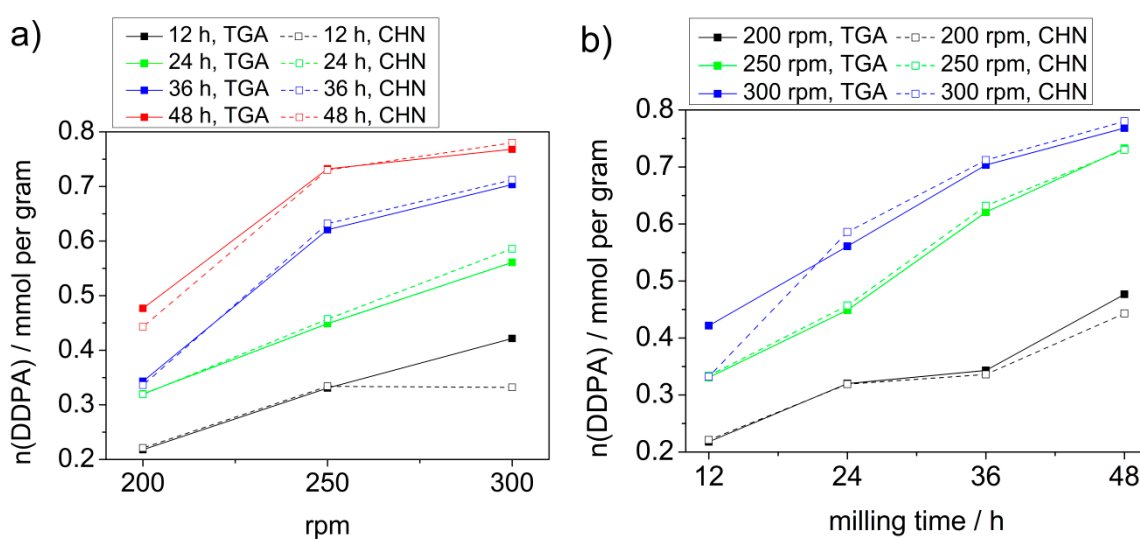


**Figure 3.** CP-MAS  $^{31}\text{P}$  (left) and  $^{13}\text{C}$  (right) spectra of titania milled with dodecylphosphonic acid at 200 rpm for 48 h.

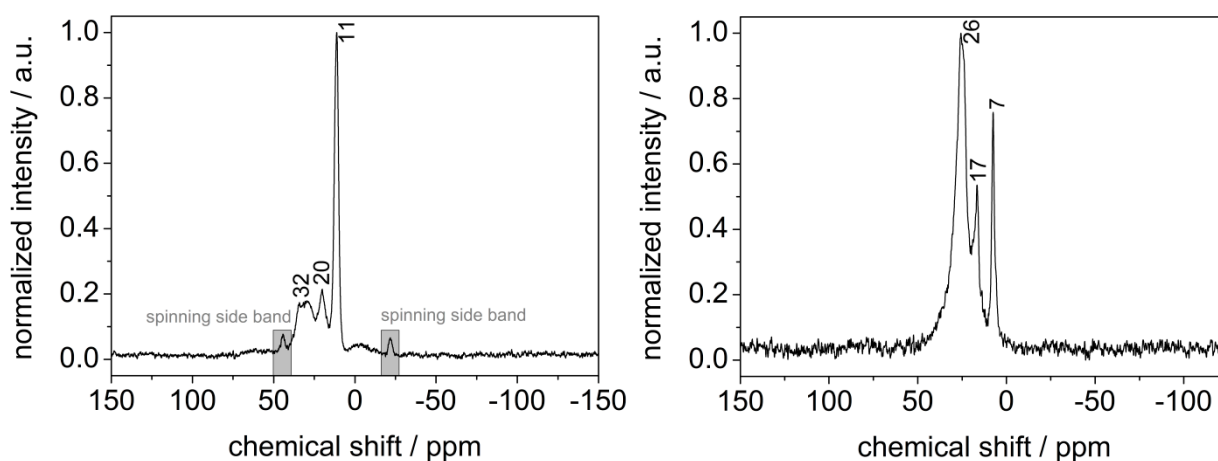
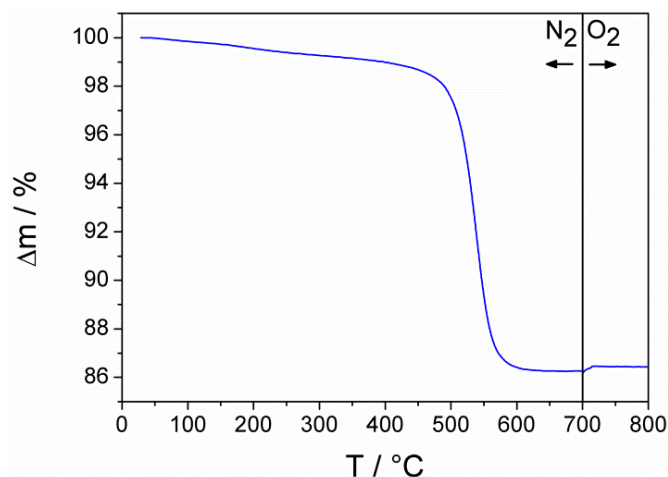
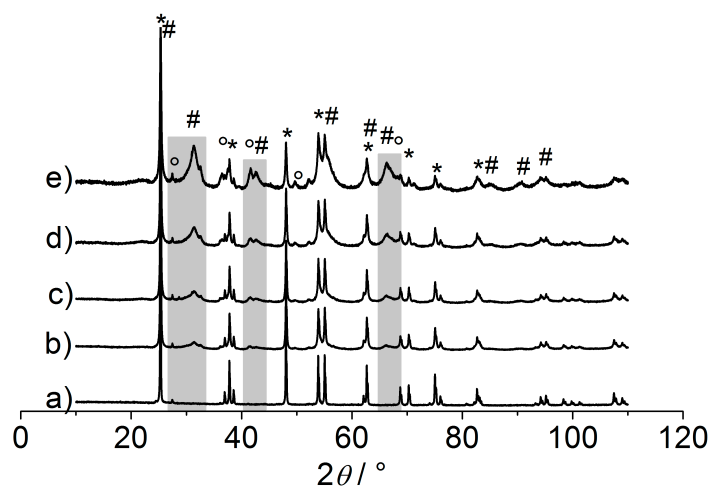


**Figure 4.** Thermal gravimetric analysis (TGA) of a sample obtained by reactive milling of titania with DDPA. All samples reveal the same TGA profile and differ only in the overall mass loss. The following figure shows the sample which was exposed to the highest energy impact (300 rpm, 48 h).



X-ray powder diffraction was used to study the phase composition of the final products. The results show that a tribochemical phase transition from the starting material anatase to the thermodynamic more stable rutile as well as a high-pressure modification of titania occurs. It turned out that the degree of the phase transition is dependent on the process parameters. The reflections belonging to the rutile and the high-pressure phase ( $2\theta = 27^\circ$  or  $31^\circ$ ,  $42^\circ$  and  $66^\circ$ , respectively) become more intensive when the milling time or the rotational speed are enhanced (Figure 5 and Supplementary Information Figures S13 and S14). The difference between the rutile and the high-pressure modification present itself in the orientation of the vertex-connected  $\text{TiO}_6$ -octahedra along the  $c$ -axis. In case of rutile, they form straight lines and in case of high-pressure titania they build zigzag chains.

**Figure 5.** XRD patterns of (a) the starting material anatase (\*) and some samples after milling with dodecylphosphonic acid (DDPA): (b) 300 rpm/12 h; (c) 300 rpm/24 h; (d) 300 rpm/36 h; (e) 300 rpm/48 h. The selection indicates the main differences in the reflections: The presence of high-pressure  $\text{TiO}_2$  (#) ( $2\theta = 31^\circ$ ,  $42^\circ$  and  $66^\circ$ ) and rutile (°) ( $2\theta = 27^\circ$ ) is indicated by additional reflections.

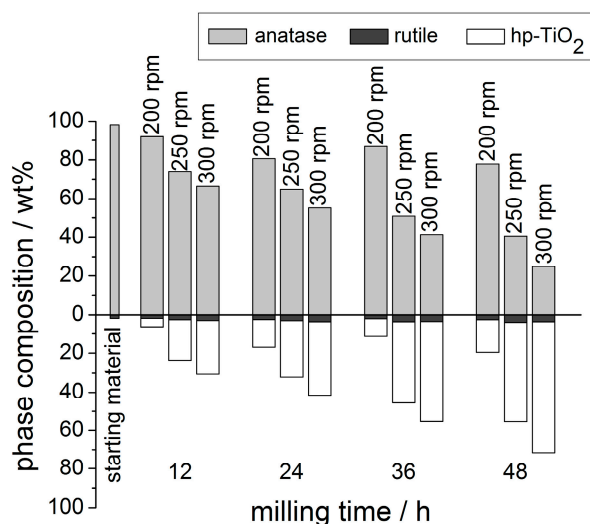


Additional to the qualitatively visible change in the reflection intensity a quantitative Rietveld phase analysis was performed. The development of the background gives no evidence for the presence of an amorphous phase. Nevertheless, the presence of such a phase cannot be excluded but if it should be present its proportion is estimated to be less than 5%. The summarized results are presented in Figure 6 and some results are listed in Table 1 (see also Supplementary Information Table S1). The Rietveld analysis confirms that the fraction of rutile and high-pressure TiO<sub>2</sub> increases with longer milling time and higher milling speed.

**Table 1.** Titania milled with dodecylphosphonic acid (DDPA), phase composition of some selected samples.

Process parameter	Anatase/wt%	Rutile/wt%	hp-TiO <sub>2</sub> /wt%
0 h/0 rpm	98.2 ± 0.1	1.8 ± 0.1	0
12 h/200 rpm	91.9 ± 0.2	1.8 ± 0.1	6.3 ± 0.2
48 h/200 rpm	77.8 ± 0.3	2.6 ± 0.1	19.6 ± 0.3
12 h/300 rpm	66.5 ± 0.2	2.9 ± 0.2	30.6 ± 0.2
48 h/300 rpm	24.9 ± 0.2	3.5 ± 0.2	71.6 ± 0.2

**Figure 6.** Titania milled with dodecylphosphonic acid (DDPA): Phase composition of the samples after the milling process determined by X-ray powder diffraction and Rietveld analysis. Phase composition occurs from the starting material anatase to rutile and high-pressure (hp) TiO<sub>2</sub>.

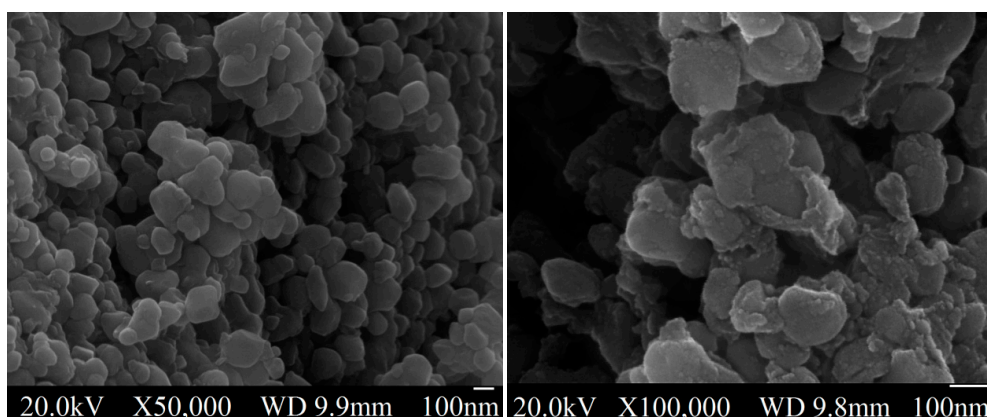


Besides the surface functionalization and phase transition, further important characteristics of the samples are the crystallite as well as the particle size. The crystallite sizes were derived from XRD pattern applying the Pawley method. The starting material was granular crystalline anatase, which exhibits crystallite sizes above 300 nm. The high-pressure TiO<sub>2</sub> formed during the milling process has crystallite sizes around 6 nm but the residual anatase phase remains in the granular crystalline dimension. Compared to the starting material there is only a reduction of about 100 nm. For the rutile phase no reliable refinement of crystallite size could be performed due to the low percentage of this phase in the mixture. These results show that the milling time and the rotational speed primarily have influence on

the phase transition but not on the particle size. Regardless of how the process parameters were selected, the resulting high-pressure TiO<sub>2</sub> is nano crystalline and the residual anatase remains as granular crystalline. Furthermore, the morphology of the obtained samples was analyzed applying SEM measurements (Figure 7). The SEM images display that the particles are not uniformly shaped and agglomerated with particle sizes in a range of 100–300 nm. It is evident that the particle size decreases with increasing milling time and rotational speed.

In order to determine the particle size, dynamic light scattering was performed. Various organic solvents such as ethanol, hexane, ethyl acetate, toluene or tetrahydrofuran were tested but, even with the use of ultrasound, it was not possible to obtain a monodisperse suspension. Consequently, in regards to the particle size, no reliable results could be obtained. This effect is characteristic for long alkyl chain functionalized particles because of the zipper effect which indicates that the surface modifying compound molecules get caught to each other due to Van-der-Waals interactions forming very stable agglomerates [20].

**Figure 7.** SEM images of two selected samples: titania milled with dodecylphosphonic acid (DDPA) at 200 rpm for 12 h (left) and at 300 rpm for 48 h (right). The size of the particles decreases with increasing energy input, but both samples are agglomerated and not uniformly shaped.



Due to abrasion of the grinding bowl, a contamination of the samples cannot be avoided but it is expected to be insignificantly small. X-ray fluorescence spectroscopy was used to analyze these impurities (Figure 8). The results confirm that the contamination of the samples due to abrasion of the grinding bowl is negligible. The contamination increases with increasing milling time and rotational speed.

The samples after the milling process show a grey discoloration which becomes more intensive with increasing milling time and speed (Figure 9). Based on the fact that starting materials, TiO<sub>2</sub> and DOPA, as well as the grinding bowl material are white, this discoloration must have another origin than the impurities due to the abrasion of the grinding bowl. Electron paramagnetic resonance was applied to clarify the reason for the mentioned discoloration (see Supplementary Information Figure S15). The results indicate the presence of Ti<sup>3+</sup> ions which are known to entail a darkening of the material [21]. An explanation for the appearance of a subvalent Ti species is the fact that the DOPA acts not only as a coupling but also as a reducing agent under the harsh conditions present during the milling process. Most likely, the organic moiety is oxidized to phenolic/chinoide species or split off



from the coupling agent molecule, respectively. However, as the concentration of  $\text{Ti}^{3+}$  is low, the amount of possible oxidation products for DDPA in the washing solution is clearly below the detection limit of NMR spectroscopy. Therefore, an identification of these side products was not successful.

**Figure 8.** Impurities introduced by the grinding bowl according to (a) rotational speed (rpm) or (b) milling time determined by X-ray fluorescence spectroscopy, titania milled with dodecylphosphonic acid.

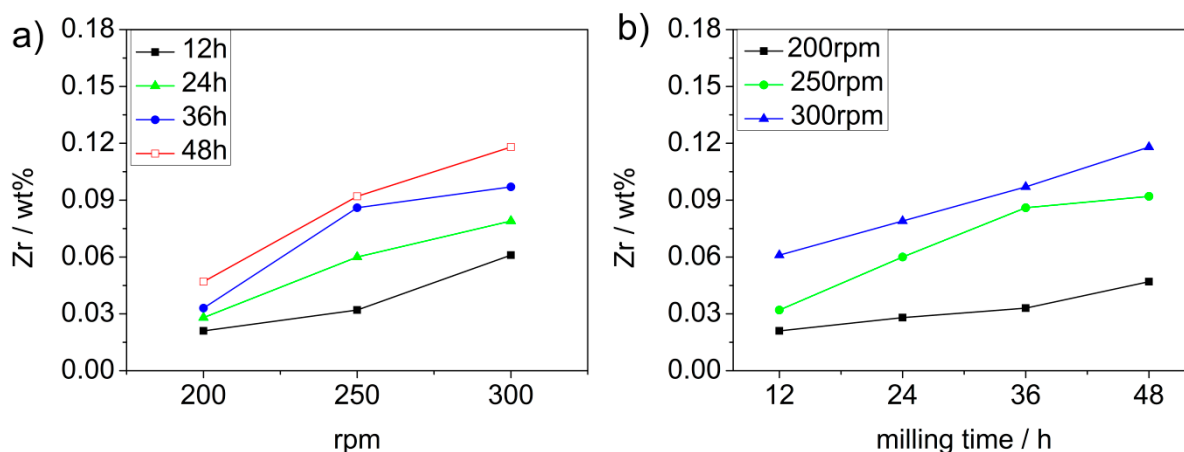
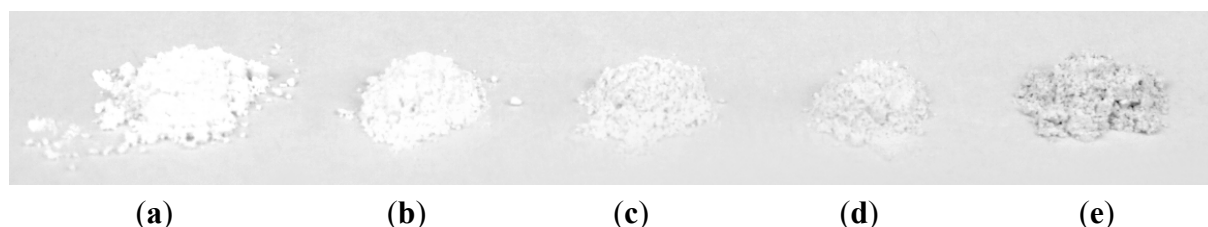


**Figure 9.** Images of some selected samples: (a)  $\text{TiO}_2$  (b) 200 rpm/12 h (c) 200 rpm/48 h (d) 300 rpm/12 h (e) 300 rpm/48 h. The grey discoloration increases with increasing energy input.



After the successful studies on DDPA as long alkyl chain phosphonate coupling agent, again ODPA was used to demonstrate that this approach is assignable on other long alkyl chain organophosphorus species. The sample was prepared in the same way using those process parameters which end up in the highest surface functionalization (300 rpm and 48 h). FTIR analysis showed that a surface functionalization has taken place in case of using ODPA as well (Figure 10). The degree of surface functionalization was determined to be 0.6 mmol/g by the use of TGA as well as CHN analysis. The binding modes of the ODPA on the titania surface were studied using solid state  $^{31}\text{P}$ -NMR spectroscopy (Figure 11). Similar to the results of the studies with DDPA, the spectrum show a series of partially broad signals in the range of  $\delta = 10\text{--}30$  ppm and a sharp peak at  $\delta = 6$  ppm. Pure ODPA shows a solid-state  $^{31}\text{P}$  NMR signal at  $\delta = 30$  ppm [22]. The  $^{31}\text{P}$  NMR is in good agreement with the variety of possible binding modes of the phosphonate to the metal oxide surface (tridentate coordination modes shift around 20 ppm to lower fields with respect to the free phosphonic acid; for bi- and monodentate binding modes a downfield shift of 5–15 ppm compared to the free acid is reported) [18]. Consequently, the peaks in the range of 10–30 ppm correspond to the bi- and monodentate bonded



phosphonates, and the sharp signal at around 6 ppm can be assigned to the tridentate coordinated species. These shifts confirm the covalent bonding of the ODPA on the titania surface and demonstrate the different binding modes. Analogous to DDPA functionalized titania, the presence of layered alkyl phosphonates can be excluded by TG measurements of the ODPA functionalized sample (Figure 12).

**Figure 10.** FTIR-spectra of the starting material, the coupling agent OPDA, and the sample after the milling process.

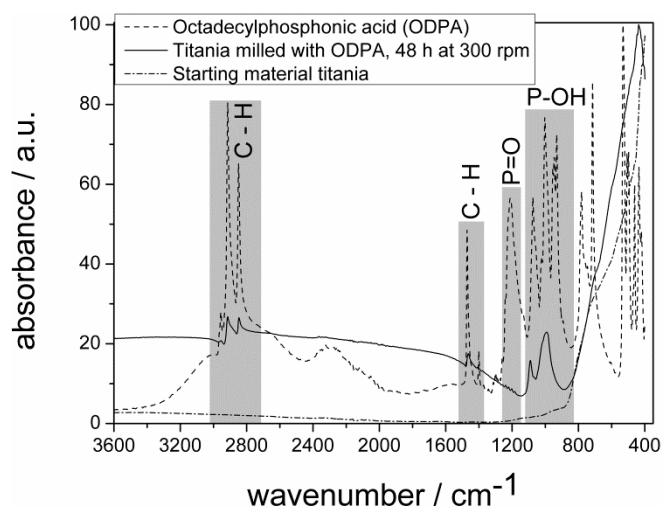


**Figure 11.** CP-MAS  $^{31}\text{P}$  NMR spectrum of titania milled with octadecylphosphonic acid.

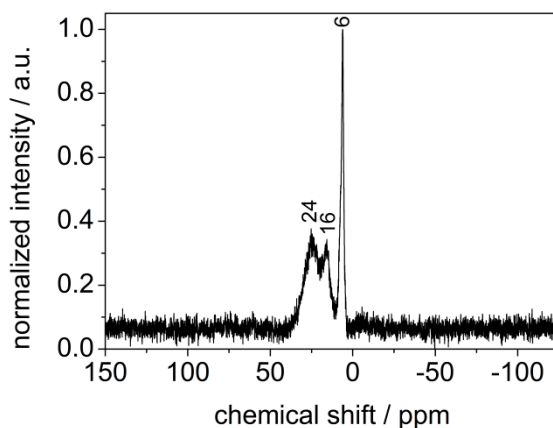
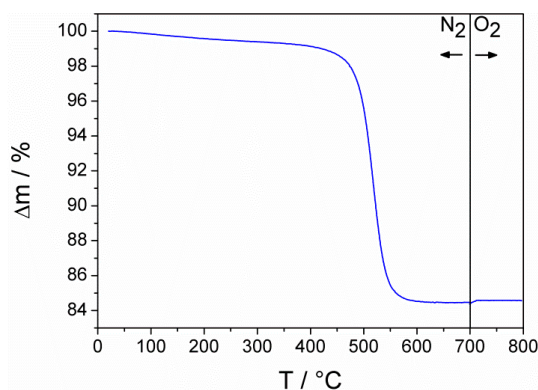
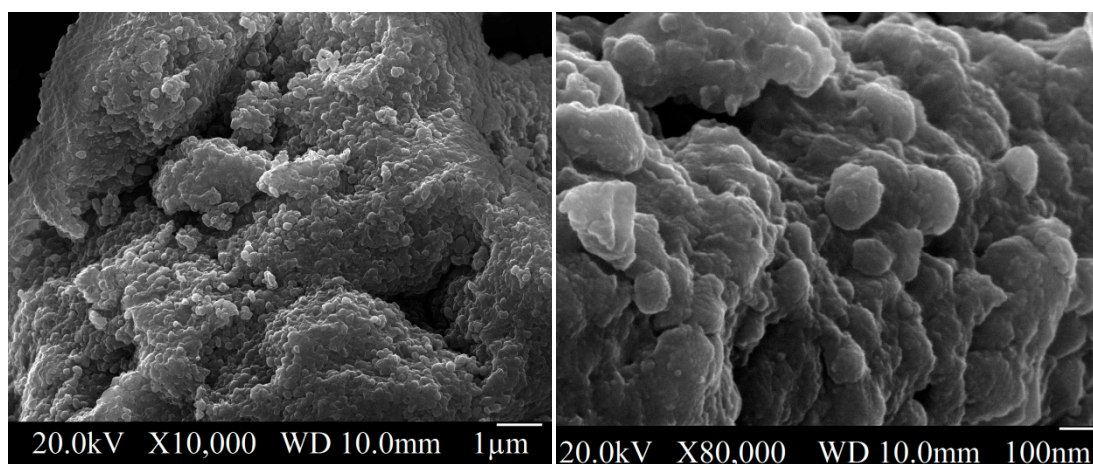


**Figure 12.** TGA of the sample obtained by reactive milling of titania with ODPA.



The sample with ODPA as coupling agent was analyzed using X-ray diffraction as well determining the phase composition or rather to describe the tribochemical phase transformation. The sample was composed of  $29.1\% \pm 0.2\%$  anatase,  $2.1\% \pm 0.2\%$  rutile and  $68.8\% \pm 0.3\%$  high-pressure  $\text{TiO}_2$ . Comparing these results with the findings of DDPA as coupling agent, it emphasizes that, in case of DDPA, a slightly higher degree of functionalization can be reached. In contrast, the degree of the tribochemical phase transformation is almost similar. Just as in the case of DDPA, the particles functionalized with ODPA are not uniformly shaped and agglomerated which was determined applying SEM techniques (Figure 13).

**Figure 13.** SEM image of titania functionalized with ODPA.



### 3. Experimental Section

#### 3.1. Materials

Titanium(IV)-oxide powder anatase (99.8%) was purchased from Sigma Aldrich (Steinheim, Germany) and has been used without further purification. Dodecylphosphonic and octadecylphosphonic acid were synthesized in the working group.

#### 3.2. Instruments and Characterization

FTIR measurements were performed under ambient air (40 scans at a resolution of  $4\text{ cm}^{-1}$ ) in attenuated total reflectance (ATR) mode on a Bruker (Billerica, MA, USA) Vertex 70 spectrometer. X-ray powder diffraction was carried out on two different diffractometers, a Panalytical (Almelo, Netherlands) X'Pert and a Bruker (Billerica, MA, USA) D8 Advance-system, and Bragg-Brentano geometry and  $\text{CuK}\alpha$  radiation was used in both cases. The quantitative analysis was carried out by the Rietveld-method using the program TOPAS [23] and crystallographic data for the modifications of titania (anatase [24], rutile [25], high-pressure  $\text{TiO}_2$  [26]). The same program package was used for the determination of the crystallite sizes applying the Pawley-method. X-ray fluorescence spectroscopy measurements were performed on an EDAX (Wiesbaden, Germany) Eagle II instrument. Thermogravimetric analysis (TGA) was carried out on a Netzsch (Selb, Germany) Iris TG 209. The sample was placed in an alumina crucible which was then heated from room temperature to  $700\text{ }^\circ\text{C}$  under nitrogen atmosphere followed by heating to  $800\text{ }^\circ\text{C}$  under oxygen atmosphere with a rate of

20 K min<sup>-1</sup>. The aim of this procedure is the removal of organic residues which were not completely decomposed during the heating step up to 700 °C. The mass loss during the thermal analysis was used to calculate the amount of coupling agent on the surface of the titania particles. Here, one has to consider that the residue is not only titania, because the phosphonate groups are oxidized to phosphate which remains on the surface of the particles. Equation 1 gives the molar amount of surface-modifying agent per gram of particles.

$$c_{CA} = \frac{\Delta m \cdot 10}{M_{\Delta m}} \quad (1)$$

$c_{CA}$ : molar concentration of surface-modifying agent per gram (mmol g<sup>-1</sup>)

$\Delta m$ : mass loss during thermal analysis (%)

$M_{\Delta m}$ : molar mass of the molecule which leaves during thermal analysis (g mol<sup>-1</sup>)

Elemental analysis was carried out on a Leco (St. Joseph, MI, USA) CHN-900 analyzer. The amount of coupling agent on the surface of the titania particles was calculated by using the percentage of carbon from elemental analysis. The molar amount of coupling agent per gram of particles can be calculated using Equation (2).

$$c_C = \frac{m_C \cdot 10}{M_C \cdot N_C} \quad (2)$$

$c_{CA}$ : molar concentration of coupling agent per gram (mmol g<sup>-1</sup>)

$m_C$ : mass of carbon from elemental analysis (%)

$M_C$ : molar mass of carbon (g mol<sup>-1</sup>)

$N_C$ : number of carbon atoms per coupling agent

Liquid state NMR spectra were recorded on a Bruker (Billerica, MA, USA) Avance 300 spectrometer operating at 300.13 MHz for <sup>1</sup>H, 75.47 MHz for <sup>13</sup>C and at 121.49 MHz for <sup>31</sup>P. Solid state NMR spectroscopy was carried out on a Bruker (Billerica, MA, USA) Avance DPX 300 instrument equipped with a 4 mm broad band cross-polarization Magic Angle Spinning probe head operating at 75.40 MHz for <sup>13</sup>C and 121.39 MHz for <sup>31</sup>P or on a Bruker (Billerica, MA, USA) DSX Avance NMR spectrometer (125.78 MHz for <sup>13</sup>C and 202.48 MHz for <sup>31</sup>P). Scanning electron microscopy (SEM) images were recorded on a JEOL (Tokyo, Japan) SEM-7000 microscope. The SEM samples were prepared by placing some grains on a specimen stub with attached carbon adhesive foil followed by deposition of a gold layer.

### 3.3. Synthesis

The experiments were performed in a high energy planetary ball mill Retsch (Haan, Germany) PM 100. The material of the grinding bowl was a ZrO<sub>2</sub>-ceramic. We used a 50 mL grinding bowl and 200 corresponding milling balls with a diameter of 5 mm. Systematic studies on the effect of the milling time and the rpm on the result of the milling process were carried out. The milling time was varied between 12 h and 48 h and the rpm had values of 200 rpm, 250 rpm and 300 rpm.

In each case, 4 g of titania (anatase) and 1 g of the respective coupling agent (dodecylphosphonic and octadecylphosphonic acid) were placed in the grinding bowl and milled at specific parameters.

After the milling process, the product was washed with ethanol and water. Finally, the functionalized particles were separated by centrifugation (13,000 rpm) and dried at 100 °C.

#### 4. Conclusions

Reactive milling can be used for the synthesis of metal oxide particles with *in situ* surface functionalization. It was shown that this technique can be successfully conducted using long alkyl chain organophosphorus coupling agents. DDPA was used to conduct systematic studies on the influence of the process parameters milling time and rotational speed. The results reveal that increasing milling time as well as increasing rotational speed results in an increasing phase transition of the starting material anatase to rutile and high-pressure titania. Furthermore, an increase of the mentioned process parameters results in an increase of surface functionalization. Afterwards, ODPA was used to successfully demonstrate that the approach is assignable on other long alkyl chain organophosphorus species. The surface functionalization of inorganic particles with long alkyl chain coupling agents is useful for further applications. For instance, such surface functionalized particles can be incorporated into a polymer matrix to obtain a composite material with improved properties. Furthermore, the approach could be conducted applying other organic coupling agents, for example antenna molecules for photo catalysis.

#### Acknowledgments

The authors thank Susanne Harling (Saarland University) for the elemental analysis and Matthias Gasthauer (Saarland University) for the synthesis of the coupling agents. Furthermore, we thank Michael Puchberger (Vienna University of Technology) and Dirk Schaffner (University of Kaiserslautern) for the solid state NMR spectroscopy and Martin Hartmann (Friedrich-Alexander University Erlangen-Nürnberg) for the ESR measurements.

#### Author Contributions

Annika Betke carried out the experiments and characterizations except elemental analysis, solid state NMR and ESR (see Acknowledgments). Guido Kickelbick provided the resources and infrastructure that allowed the development of this work. He also provided mentoring with data analysis and sample characterization. All co-authors compiled and discussed the manuscript.

#### Conflicts of Interest

The authors declare no conflict of interest.

#### References

1. Hameed, S.; Predeep, P.; Baiju, M.R. Polymer Light Emitting Diodes—A Review on Materials and Techniques. *Rev. Adv. Mater. Sci.* **2010**, *26*, 30–42.
2. Chen, W.; Qiu, Y.; Yang, S. Branched ZnO nanostructures as building blocks of photoelectrodes for efficient solar energy conversion. *Phys. Chem. Chem. Phys.* **2012**, *14*, 10872–10881.

3. Leung, K.C.-F.; Xuan, S.; Zhu, X.; Wang, D.; Chak, C.-P.; Lee, S.-F.; Ho, W.K.-W.; Chung, B.C.-T. Gold and iron oxide hybride nanocomposite materials. *Chem. Soc. Rev.* **2012**, *41*, 1911–1928.
4. Mieszawska, A.J.; Mulder, W.J.M.; Fayad, Z.A.; Cormode, D.P. Multifunctional Gold Nanoparticles for Diagnosis and Therapy of Disease. *Mol. Pharm.* **2013**, *10*, 831–847.
5. Fernández-Bertran, J.F. Mechanochemistry: An overview. *Pure Appl. Chem.* **1999**, *71*, 581–586.
6. Garay, A.L.; Pichon, A.; James, S.L. Solvent-free synthesis of metal complexes. *Chem. Soc. Rev.* **2007**, *36*, 846–855.
7. Kaupp, G. Waste-free large-scale synthesis without auxiliaries for sustainable production omitting purifying workup. *CrystEngComm* **2006**, *8*, 794–804.
8. James, S.L.; Adams, C.J.; Bolm, C.; Braga, D.; Collier, P.; Friscic, T.; Grepioni, F.; Harris, K.D.M.; Hyett, G.; Jones, W.; *et al.* Mechanochemistry: Opportunities for new and cleaner synthesis. *Chem. Soc. Rev.* **2012**, *41*, 413–447.
9. Ney, C.; Kohlmann, H.; Kickelbick, G. Metal hydride synthesis through reactive milling of metals with solid acids in a planetary ball mill. *Int. J. Hydrogen Energy* **2011**, *36*, 9086–9090.
10. Fuentes, A.F.; Takacs, L. Preparation of multicomponent oxides by mechanochemical methods. *J. Mater. Sci.* **2013**, *48*, 598–611.
11. Fischer, A.; Ney, C.; Kickelbick, G. Synthesis of Surface-Functionalized Titania Particles with Organophosphorus Coupling Agents by Reactive Milling. *Eur. J. Inorg. Chem.* **2013**, *33*, 5701–5707.
12. Betke, A.; Kickelbick, G. Important reaction parameters in the synthesis of phenylphosphonic acid functionalized titania particles by reactive milling. *New J. Chem.* **2014**, *38*, 1264–1270.
13. Guerrero, G.; Mutin, P.H.; Vioux, A. Anchoring of Phosphonate and Phosphinate Coupling Molecules on Titania Particles. *Chem. Mater.* **2001**, *13*, 4367–4373.
14. Convertino, A.; Leo, G.; Tamborra, M.; Sciancalepore, C.; Striccoli, M.; Curri, M.L.; Agostiano, A. TiO<sub>2</sub> colloidal nanocrystals functionalization on PMMA: A tailoring of optical properties and chemical adsorption. *Sens. Actuators B* **2007**, *126*, 138–143.
15. Cozzoli, P.D.; Kornowski, A.; Weller, H. Low-Temperature Synthesis of Soluble and Processable Organic-Capped Anatase TiO<sub>2</sub> Nanorods. *J. Am. Chem. Soc.* **2003**, *125*, 14539–14548.
16. El Malti, W.; Laurencin, D.; Guerrero, G.; Smith, M.E.; Mutin, P.H. Surface modification of calcium carbonate with phosphonic acids. *J. Mater. Chem.* **2012**, *22*, 1212–1218.
17. Brodard-Severac, F.; Guerrero, G.; Maquet, J.; Florian, P.; Gervais, C.; Mutin, P.H. High-Field <sup>17</sup>O MAS NMR Investigation of Phosphonic Acid Monolayers on Titania. *Chem. Mater.* **2008**, *20*, 5191–5196.
18. Pica, M.; Donnadio, A.; Troni, E.; Capitani, D.; Casciola, M. Looking for New Hybrid Polymer Fillers: Synthesis of Nanosized  $\alpha$ -Type Zr(IV) Organophosphonates through an Unconventional Topotactic Anion Exchange Reaction. *Inorg. Chem.* **2013**, *52*, 7680–7687.
19. Souma, H.; Chiba, R.; Hayashi, S. Solid-State NMR Study of Titanium Dioxide Nanoparticles Surface-Modified by Alkylphosphonic Acids. *Bull. Chem. Soc. Jpn.* **2011**, *84*, 1267–1275.
20. Bedia, A.; Cuccia, L.; Demers, L.; Morin, F.; Lennox, R.B. Structure and Dynamics in Alkanethiolate Monolayers Self-Assembled on Gold Nanoparticles: A DSC, FT-IR, and Deuterium NMR Study. *J. Am. Chem. Soc.* **1997**, *119*, 2682–2692.

21. Xiong, L.-B.; Li, J.-L.; Yang, B.; Yu, Y.  $Ti^{3+}$  in the Surface of Titanium Dioxide: Generation, Properties and Photocatalytic Application. *J. Nanomater.* **2012**, *2012*, 13, doi.org/10.1155/2012/831524.
22. Tienes, B.M.; Perkins, R.J.; Shoemaker, R.K.; Dukovic, G. Layered Phosphonates in Colloidal Synthesis of Anisotropic ZnO Nanocrystals. *Chem. Mater.* **2013**, *25*, 4321–4329.
23. *Topas*, V4.2; General Profile and Structure Analysis Software for Powder Diffraction Data, User Manual; Bruker AXS: Karlsruhe, Germany, 2008.
24. Kim, D.-W.; Enomoto, N.; Nakagawa, Z.; Kawamura, K. Molecular Dynamic Simulaion in Titanium Dioxide Polymorphs: Rutile, Brookite, and Anatase. *J. Am. Ceram. Soc.* **1996**, *4*, 1095–1099.
25. Hill, R.J.; Madsen, C. Rietveld analysis using para-focusing and Debye-Scherrer geometry data collected with a Bragg-Brentano diffractometer. *Z. Kristallogr.* **1991**, *196*, 73–92.
26. Fulatov, S.K.; Bendeliani, N.A.; Albert, B.; Kopf, J.; Dyuzheva, T.; Lityagina, L.M. Crystalline structure of the  $TiO_2$  II high-pressure phase at 293, 223, and 133 K according to single-crystal x-ray diffraction data. *Dokl. Phys.* **2007**, *52*, 195–199.

© 2014 by the authors; licensee MDPI, Basel, Switzerland. This article is an open access article distributed under the terms and conditions of the Creative Commons Attribution license (<http://creativecommons.org/licenses/by/3.0/>).